ACTA UNIVERSITATIS AGRICULTURAE ET SILVICULTURAE MENDELIANAE BRUNENSIS

Volume 67 123 Number 6, 2019

TOWARDS AN UNDERSTANDING OF SPECIFIC RESPONSE OF METALLOTHIONEIN (SUB)ISOFORMS TO EXPOSURE TO PLATINUM-BASED ANTICANCER DRUGS

Sofie Blížkovská[1]

[1] Department of Chemistry and Biochemistry, Mendel University in Brno, Zemědělská 1, 613 00 Brno, Czech Republic

To link to this article: https://doi.org/10.11118/actaun201967061407
Received: 10. 9. 2019, Accepted: 31. 10. 2019

To cite this article: BLÍŽKOVSKÁ SOFIE. 2019. Towards an Understanding of Specific Response of Metallothionein (Sub)Isoforms to Exposure to Platinum-Based Anticancer Drugs. *Acta Universitatis Agriculturae et Silviculturae Mendelianae Brunensis,* 67(6): 1407–1417.

Abstract

Metallothioneins (MTs) are small cysteine-rich proteins involved in a number of pathophysiological processes. Particularly their linkage to cancer processes has been vastly studied and it is well known that MTs can inactivate metal-based cytostatics or scavenge free radicals. These processes result in pronounced chemoresistance and a poor prognosis for patients. Despite this knowledge, involvement of specific (sub)isoforms into this phenomenon requires further elucidation. Our results identified CisPt as the cytostatic which provoked the highest cell death exp followed by CarboPt and OxaliPt. Fluorescence microscopy visualized the oxidative cell stress. After application of 24hIC_{50} values, the reactive oxygen species (ROS) were visually produced. Our results also showed that MT 1, 2 and 3 expression manifested the highest qPCR activity after CisPt treatment (both healthy and cancer cells). While evaluating the expression of the protein level in the healthy and cancer cells treated by the cytotoxics we concluded that for MT1 and MT3 it was low under all three cytostatic treatments. Cancer cells had higher protein expression levels than healthy cells. In case of MT1/2 for cancer cells was highest under CisPt treatment.

Keywords: Cancer treatment, metal-based cytostatic, metallothioneins, mRNA and protein expression, qPCR activity

INTRODUCTION

Literature Overview

Metallothioneins and their isoforms

Metallothioneins (MTs) were originally discovered as proteins binding cadmium and zinc which led to their name (Krężel and Maret, 2007). MTs are small cystein-rich proteins that protect the host cell against toxic heavy metals. MTs are commonly present throughout all kingdoms. Their main physiological function is to neutralize free radicals in order to prevent cells from toxic environment and thus homeostate heavy metals. MTs also protect cells from DNA damage and oxidative stress. They contribute to tissue repair, modulate immune responses and limit inflammatory processes (McGee, Woods, Bennett and Chung, 2010). According to Krizkova *et al*., 2018: *'In humans, 16 genes localized on chromosome 16 have been identified to encode four MT isoforms labeled by numbers (MT-1–MT4). MT-2, MT-3 and MT-4 proteins are encoded by a single gene. MT-1 comprises many (sub)isoforms.'* The most widely expressed isoforms in the body are MT1 and MT2. MT2a appears to be expressed more in human

tissues than MT1. MT3 is found mainly in brain, but is also expressed in tongue, stomach, heart, kidney and reproductive tissues (Coyle, Philcox, Carey *et al*., 2002). In humans, 11 functional members of MT1 have been identified (Si and Lang, 2018).

Metallothioneins and their interaction with cancer

MTs play a key role in cancerogenic processes. Firstly, due to the MT's affinity for heavy metals, they can control the cellular homeostasis of zinc and copper, which is essential for cell proliferation. MTs function as antioxidants to protect cells against free radicals and oxidative stress. Such a stress is produced by mutagens, antineoplastic drugs and radiation. Secondly, MTs care also bind other heavy metals such as cadmium, mercury and platinum to shelter cells and tissues against heavy metals toxicity. MTs are able to bind up to 20 monovalent and up to 7 divalent heavy metal ion (Krizkova *et al.*, 2016). Thirdly, MTs defend cells against DNA damage and apoptosis (Si and Lang, 2018). Therefore, MTs are involved in tumor growth through cell cycle, cell proliferation and cell apoptosis. Next, MTs play role in tumor metasastasis via tumor cell adhesion, invasion, migration and through tumor microenvironment remodelling. MTs also cause tumor differentiation because they are involved in cell signalling pathway, zinc chelation and zinc distribution. Finally, MTs create immunomodulation through regulation, homeostasis and inhibition of human response. Krizkova *et al.* (2016) summarize expression and regulation of individual MT isoforms with several types of malignancies. After comparing the transcription levels of MTs to those in normal samples, the results showed that mRNA levels of MT isoforms are significantly up/downregulated in various types of cancers.

Metallothioneins and their interaction with metal-based cancer drugs

The interaction of MTs with metal-based cancer drugs has been widely studied (Zalewska *et al.*, 2014). Metal-based antitumor inorganic drugs are successfully used in cancer treatment. One of the most commonly used drugs is cisplatin (*cis*-diamminedichlorplatinum). It is effective in treating advanced testicular cancers and ovarian cancers with cure rates of about 90% and 70%, respectively. Together with other Pt-based drugs, cisplatin (CisPt), carboplatin (CarboPt) and oxaliplatin (OxaliPt), manifested a wide spectrum of antitumor functions, such as cancer of lung, bladder, breast, colon, head and neck. Pt-based drugs can attack various cellular targets including the plasma membrane, mitochondria, endo-lysosomes, endoplasmic reticulum and cytoskeleton. In addition, the Pt-based drugs are causing cell lethality due to DNA damage (Lai *et al.*, 2018).

Merlos Rodrigo *et al.* (2017) conclude that cisplatin inducts cytotoxic cell death through apoptotic mechanism and via mitochondrial pathways. Cisplatin interacts both with DNA and with proteins. It is generally accepted that damage to cytoplasmatic proteins is an early process that initiate cisplatin-induced apoptosis. It has been observed that the concentration of MTs increases once the platinum-based drug was implemented. The increase of MTs' presence in malignant cells can therefore rapidly bind the applied cisplatin. This mechanism results in the decrease of the drug concentration below the effective level. Thus, MTs can inhibit the platinum-based cancer drug (Merlos Rodrigo *et al.*, 2017). MTs are suspected to interfere with the metal-based drugs through ligand removal and metal sequestration. Wong and Stillman (2018) studied the mechanistic details and deconstruction of cisplatin by human MTs. Skowron *et al.* (2018) report on cisplatin resistance in long term treatment on cancer cell lines and observed the complexity of cisplatin resistance mechanisms even within one tumor entity. Long-term cisplatin treated cells recovered rapidly from cisplatin stress compared to parental cells for instance. The expression of DNA repair factors and specific anti-apoptotic activity was elevated which demonstrates the dynamic character of cisplatin effects on treated cells.

Similarly to toxic metals, like platinum, the MTs are also involved in metabolism of essential metals, such as zinc and copper. They are binding metal ions through thiol reactivity. The buffering functions of MTs for essential metals may interact with cancer antibodies. Hence, as the metamorphic nature of the protein with structures depending on metal load may prevent the development from such antibodies (Krężel and Maret, 2017).

Metallothioneins' role in cancer diagnosis

MTs can be used as an enriched source of biomarkers. They can be detected in patient's blood, and the level of serum MTs is positively correlated with the pathological state, disease stage, and degree of cancer progression. Si and Lang (2018) and Petrlova *et al.* (2006) describe various electroanalytical techniques to detect MTs in human serum. MTs can also be utilized for diagnosis of tumor diseases. The reason is that the expression and localization of individual MTs (sub)isoforms and pseudogenes vary at intra-cellular level and in individual tissues. As conclude Krizkova *et al.* (2018), *'changes in MT expression are associated with the process of carcinogenesis of various types of human malignancies, or with a more aggressive phenotype and therapeutic resistance'.* Krizkova *et al.* (2012) provide an overview of the expression of MTs in ontogenesis and cancer prognosis. The role of MTs is linked to the presence of zinc. They conclude that MTs capture a potential for cancer diagnosis and therapy.

The above overview of the MTs involvement in cancer control, diagnosis and treatment indicate that MTs play a critical role in almost all aspects of cancer. They therefore provide an opportunity for development of MTs in understanding, novel diagnostic/prognostic techniques as well as the cancer treatment.

MATERIALS AND METHODS

Cells lines and cell culturing

Two cell lines were used in this project, human healthy keratinocytes HaCaT and human melanoma A-375. HaCaT are spontaneously transformed aneuploidy immortal keratinocyte cell lines, established from the skin of a Caucasian 62-year-old male. They were purchased from Addex Bio (San Diego, CA, USA). A-375 (ATCC CRL-1619™) originated from hypotriploid malignant melanoma of 54-year-old female. They were purchased from American Type Culture Collection (Manassas, VA, USA). Both cell lines were cultured in DMEM medium, supplemented with 10% foetal bovine serum and antibiotics (100 U/ml penicillin and 100 µg/ml streptomycin) at 37 °C with 5% CO_2.

Pt derivatives treatment

CisPt and CarboPt were purchased from Sigma Aldrich (St. Louis, MO, USA) and solubilized in 0.9% NaCl. Oxaliplatin was purchased as a ready-to-use solution from Teva Pharmaceutical Industries (Petah Tikva, Israel). To test the cytotoxicity of these compounds, MTT (3-(4,5-dimethylthiazol-2-yl)-2,5-diphenyltetrazolium bromide) assay was performed. Briefly, the suspension of 5,000 A-375 cells in 50 µl medium was added to each well of 96 well plate and cells were seeded overnight. 50 µl of medium containing platinum-based drugs (ranging in concentrations between 6 mM and 6 µM) was added to the cells, followed by incubation for 24 h at 37 °C with 5% CO_2 to ensure cell growth. After the treatment, 10 µl of MTT [5 mg/ml in phosphate buffered saline (PBS)] was added to the cells and the mixture was incubated for approx. 4 h at 37 °C. After that, MTT-containing medium was replaced by 100 µl of 99.9% dimethyl sulfoxide (DMSO) and, after 5 min incubation, absorbance of the samples was determined at 570 nm using Infinite 200 PRO (Tecan, Männedorf, Switzerland). Viability of the cells was calculated and used to determine 24hIC_{50} of each compound.

Fluorescence microscopy of reactive oxygen species (ROS)

Reactive oxygen species (ROS) are a family of molecules that are continuously generated, transformed and consumed in all living organisms as a consequence of aerobic life. The traditional view of these reactive oxygen metabolites is one of oxidative stress and damage that leads to decline of tissue and organ systems in aging and disease. However, emerging data show that ROS produced in certain situations can also contribute to physiology and increased fitness. This Perspective provides a focused discussion on what factors lead ROS molecules to become signal and/or stress agents, highlighting how increasing knowledge of the underlying chemistry of ROS can lead to advances in understanding their disparate contributions to biology. An important facet of this emerging area at the chemistry-biology interface is the development of new tools to study these small molecules and their reactivity in complex biological systems (Dickinson and Chang, 2011).

150,000 A-375 and HaCaT cells was seeded into each well of 24-well plate and cultivated overnight. Then, cells were treated by 24hIC_{50} of CisPt, OxaliPt and CarboPt cytostatics (see above) in medium, followed by cultivation for 6 h. Live cells were washed with 200 µL of phosphate buffered saline (PBS) and stained with Hoechst 33342 (nuclei counterstaining) and CellROX Green (ROS level) stains (both purchased from Thermo Fisher Scientific, Waltham, MA, USA) in dilution of 1:2,000 and 1:500, respectively, and the cells were incubated for 30 minutes. Again, cells were washed 3× with 200 µL of PBS. Cells were visualized using the EVOS FL Auto Cell Imagining System (Thermo Fisher Scientific). For visualization of nuclei, excitation of 350 nm and emission of 470 nm was used. For visualization of oxidative stress, excitation of 488 nm and emission of 510 nm was used.

Isolation RNA and Quantitative real-time polymerase chain reaction (qPCR)

500,000 A-375 and HaCaT cells was seeded into each well of a 6-well plate overnight. Then, the cells were treated by 24hIC_{50} of CisPt, OxaliPt and CarboPt cytostatics (see above) in medium, followed by cultivation for 24 h. Total RNA was isolated from the cultured cells by High Pure RNA Isolation Kit (Roche, Basel, Switzerland) according to manufacturer‘s instruction. 500 ng of total RNA was reverse-transcribed into cDNA using Transcriptor First Strand cDNA Synthesis Kit (Roche, Basel, Switzerland) in the presence of random hexamer primers. qPCR was performed using SYBR™ Select Master Mix (Sigma-Aldrich, St. Louis, MO, USA) on the Mastercycler® ep realplex 4 instrument (Eppendorf, Hamburg, Germany). Each 20 µL qPCR reaction mix was composed of 25 ng cDNA, 1xSYBR green mix and set of primers with 0.250 µM final concentration. The PCR program was carried out as follows: initial denaturation at 95 °C for 5 minutes; 40 cycles of denaturation at 95 °C for 15 s, annealing 60 °C for 15 s, extension at 68 °C for 20s. The fluorescence was measured in real-time, accordingly. To verify the specificity of the amplification reaction, high resolution melting curve analysis was performed.

Threshold levels for each experiment were set during the exponential phase of the qPCR reaction by noise band algorithm with automatic baseline drift correction performed by Realplex software (Eppendorf, Hamburg, Germany). The relative quantity of the *metallothioneins (MT1A, MT2A, MT3)* were normalized against the reference gene, *glyceraldehyde 3-phosphate dehydrogenase (GAPDH)*. Fold change differences were determined using the 2-ΔΔCT method compared with untreated cells (Livak and Schmittgen, 2001; Buchtelova *et al.*, 2018). Sequences of all primers used in qPCR analyses are listed in Tab. I and Tab. II shows the Livak method calculation of Fold Change in MT 1, 2 and 3 expression.

I: *List of primers*

Gene		primer (5´-3´)	product size (bp)
MT1A	F	TCTGCAAAGGGGCATCAGAG	122
	R	TGGGTCAGGGTTGTATGGAA	
MT2A	F	CTCGTCCCGGCTCTTTCTA	101
	R	GAGTCGGGACAGGTTGCAC	
MT3	F	TCGACATGGACCCTGAGACC	141
	R	CACACTTCTCACACTCCGCA	
GAPDH	F	AGGGCTGCTTTTAACTCTGGT	206
	R	CCCCACTTGATTTTGGAGGGA	

II: *Livak method calculation of Fold Change in metallothionein 1, 2 and 3 expression*

Calculations	
Ct	treshold cycle
ΔCt(deltaCt)	dCt = Ct GOI (MT1,2,3) - Ct reference gene (GAPDH)
ΔΔCt(deltadeltaCt)	ddCt = dCt treatment (cisPt, oxaliPt, carboPt) - dCt (Control-z_C, n_C)
Fold Change	2^-(ΔΔCt)

Western blotting

Total cellular proteins were extracted with 100 µl of RIPA buffer containing protease inhibitor cocktail for 45 min on ice, followed by centrifugation at 15,000 rcf and 4 °C for 45 min to remove cell debris. 10 µl of the lysed proteins was separated using 12.5% SDS PAGE, run at 200 V and 4 °C for 35 min. After electrophoresis, the proteins were electro-transferred onto a polyvinylidene fluoride membrane and a nonspecific binding was blocked with 5% bovine serum albumin (BSA) diluted in PBS for 30 min at 20 °C and 600 rpm. Membranes were incubated with primary mouse anti-MT1 (dilution 1:200 in 1 mg/ml BSA in PBS), biotinylated mouse anti-MT1/2 (1:500), rabbit anti-MT3 (1:250), mouse anti-GAPDH (1:700) overnight at 4 °C. After washing, membranes were incubated with anti-mouse horseradish peroxidase (HRP)-labelled secondary antibody (1:5,000, Dako, Santa Clara, CA, USA) for GAPDH and MT1, anti-rabbit HRP-labelled secondary antibody (1:5,000) for MT3 or streptavidin-conjugated HRP (1:35,000 in PBS-T) for 1 h at 20 °C. Signals were developed using Clarity Western ECL Blotting Substrate (Bio-Rad, Hercules, CA, USA) and blots were visualized using Azure c600 imager (Azure Biosystems, Dublin, CA, USA) (Buchtelova *et al.*, 2018).

Statistical analysis

To assess the results, the standard statistical methods were used: mean, standard deviation, *t*-test. StatSoft, Tulsa, OK, USA was taken to execute the statistical analysis.

RESULTS AND DISCUSSION

We ran the following tests to evaluate the effect of platinum-based cytotoxics on MTs.

Treatment with Pt derivates – Cytotoxic assay (MTT) to obtain 24hIC_{50} values

Three Pt derivates were tested in order to obtain 24hIC50 values. For the first drug, CisPt, the Fig. 1 shows a steep decrease of cell viability in a low-concentration interval followed by a more stable cell-survival pattern with increasing drug concentration. The 24hIC50 value was reached at 11 µM.

A similar test ran for OxaliPt demonstrated a different cell-viability response (Fig. 2), namely slowly declining cell viability till concentration range of 1500 µM followed by a less pronounced cell viability decline. The 24hIC_{50} value was reached at 1149 µM.

CarboPt provoked steep cell mortality till the range approximately 400 µM and with further increasing the drug concentration, the cell viability persisted more (Fig. 3). The 24hIC_{50} value was reached at 345 µM.

The comparison of results of the three Pt-based cytostatics on cell viability is shown in Fig. 4. The main result consists on the establishment of the 24hIC_{50} values. The CisPt proven to be the drug which was the first to touch the 24hIC_{50} value followed by CarboPt and finally by OxaliPt. Therefore, CisPt can be ranked as the most toxic drug, CarboPt in the second place and OxaliPt in the last position.

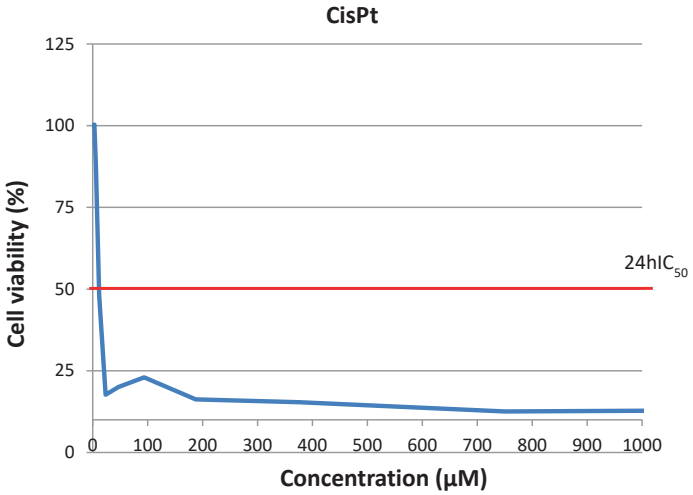

1: *Cytotoxic assay (MTT) of CisPt*

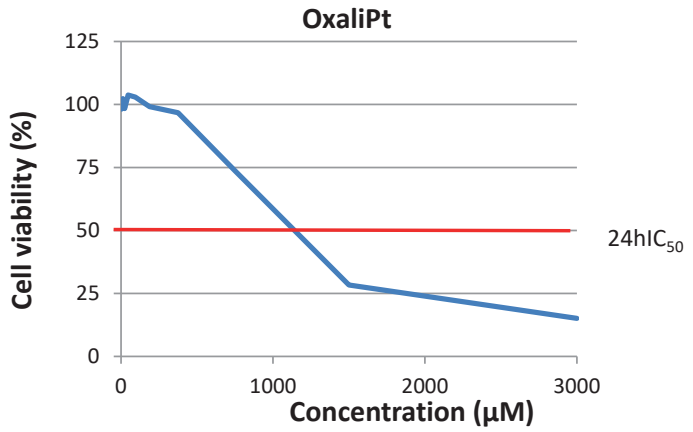

2: *Cytotoxic assay (MTT) of OxaliPt*

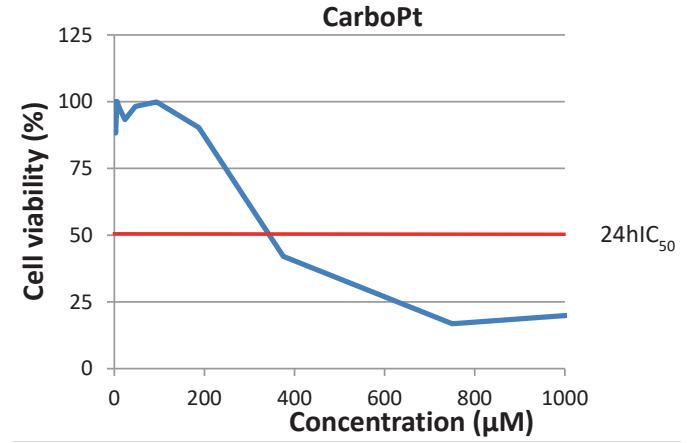

3: *Cytotoxic assay (MTT) of CarboPt*

Fluorescence microscopy of free radicals formation

The second experiment aimed at visual expression of the healthy and cancer cells after application of $24hIC_{50}$ values. We expected that reactive oxygen species (ROS) would be visually expressed due to oxidative stress which would lead to decline of tissue and organ systems after exposing drugs. The results of the fluorescence microscopy are summarized in Fig. 5.

The results show that in the healthy cells the ROS were created in the nuclei of cells treated by $24hIC_{50}$

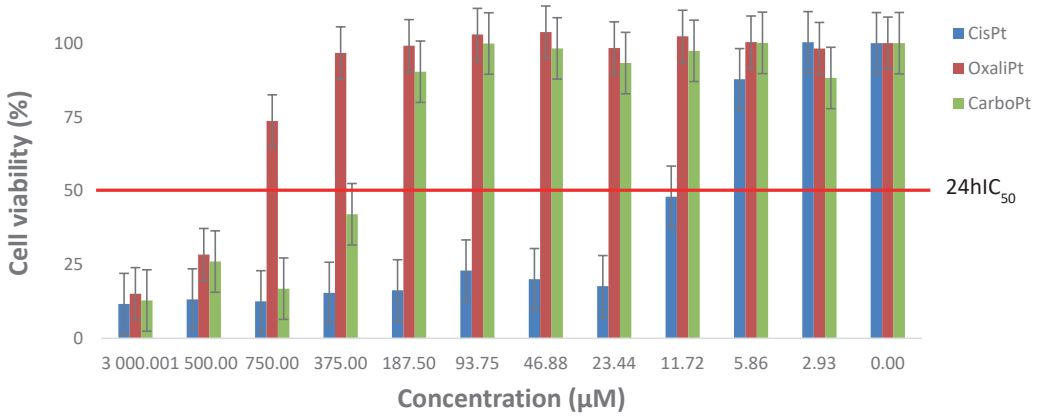

4: *24hIC$_{50}$ values Cytotoxic assay (MTT) of CisPt, OxaliPt and CarboPt*

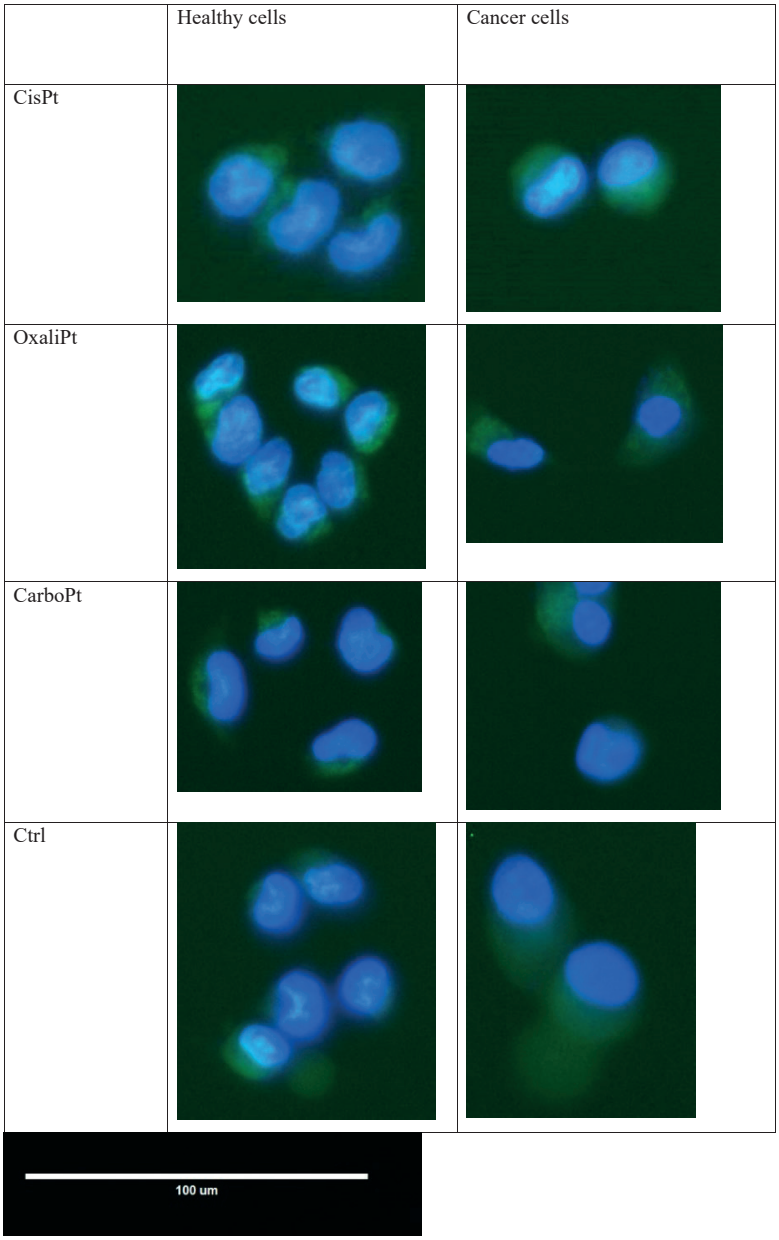

5: *Fluorescence microscopy images of healthy and cancer cells after exposing CisPt, OxaliPt and CarboPt at 24hIC50 concentration*

of CisPt and OxaliPt, not CarboPt (see green spots representing stressed ROS cells). However, in the cancer cells the ROS appeared in the nuclei in the cells treated by 24hIC_{50} of CisPt only.

As you can see in Fig. 5 by the amount and intensity of green spots around the blue nuclei, CisPt and OxaliPt-treated cells are most stressed. CarboPt-treated cells and the control, untreated cells are a little bit less stressed. Cancer cells tend to demonstrate more intense green spots, therefore, being more stressed.

qPCR – study of expression of mRNA encoding MT (sub)isoforms

To identify the effects of three Pt-based cytostatics, we tested the quantification of expression of three metallothionein isoforms, namely metallothionein 1, metallothionein 2 and metallothionein 3 in healthy and cancer cells exposed to 24hIC_{50} of CisPt, OxaliPt and CarboPt. For this purpose, qPCR was used, and the changes in expression levels are shown as Fold Change, calculated using Livak method.

Because of the different response of cancer cells to the platinum drug-based treatment, these cells have higher expression of all metallothionein isoforms in response to almost every metal than healthy cells.

Starting with metallothionein 1, Fig. 6A shows that the expression was highest in case of CisPt treatment (both healthy and cancer cells). For healthy cells, it was followed by CarboPt and OxaliPt which induced the lowest overexpression of metallothionein 1. On the other hand, for cancer cells, OxaliPt provoked higher overexpression of metallothionein 1 than CarboPt.

As we can see in Fig. 6B, for metallothionein 2, expression patterns for cancer cells are identical as in the case of metallothionein 1, meaning CisPt provoked the highest expression, followed by OxaliPt and CarboPt. For healthy cells, the expression was also highest in CisPt, with OxaliPt on second place and CarboPt at last.

The qPCR activity for metallothionein 3 is presented in Fig. 6C. Cancer cells had the highest metallothionein 3 expression under CisPt treatment followed by OxaliPt and CarboPt. While metallothionein 3 expression in healthy cells was highest in OxaliPt treatment, CisPt and CarboPt provoked similar activity level.

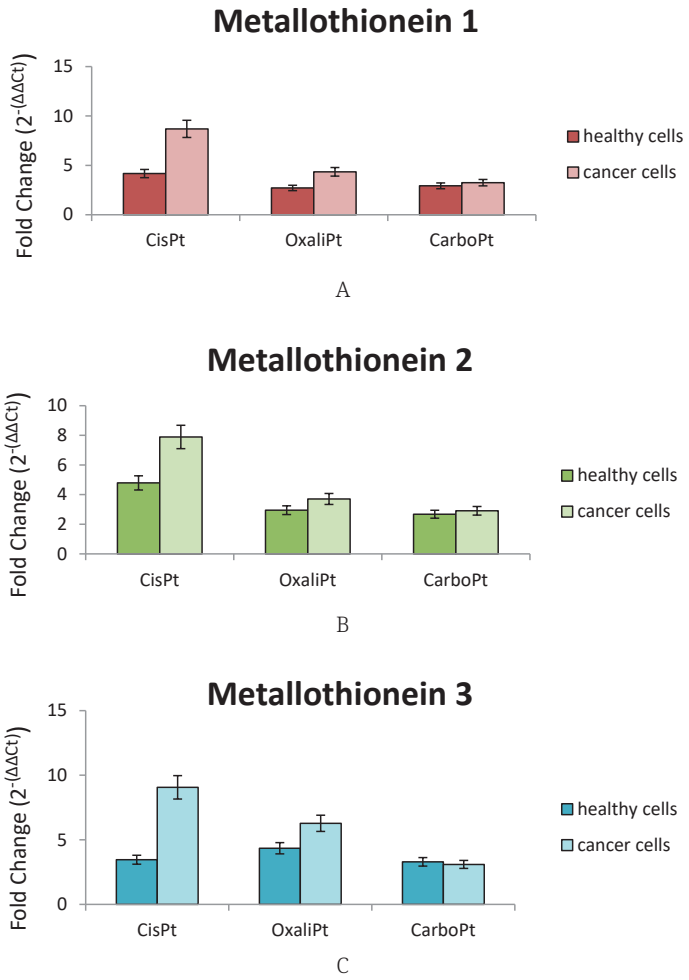

6: *Quantification of metallothionein 1 (A), 2 (B) and 3 (C) isoform expression on the mRNA level*

It is worth mentioning that generally, the platinum drug-induced overexpression of all metallothionein isoforms in cancer cells was higher compared to the one in the healthy cells. The only exception from this pattern represents the CarboPt treatment effects on metallothionein 3.

Western blotting – study of expression of proteins

The fourth test focused on the expression of the protein level. MT1, MT1/2 and MT3 were compared to control expression of Glyceraldehyde 3-phosphate dehydrogenase (GAPDH), see Fig. 7.

The results show that for MT1 (Fig. 7A), the expression at protein level under all three cytostatic treatments were low (below 1 MT1/

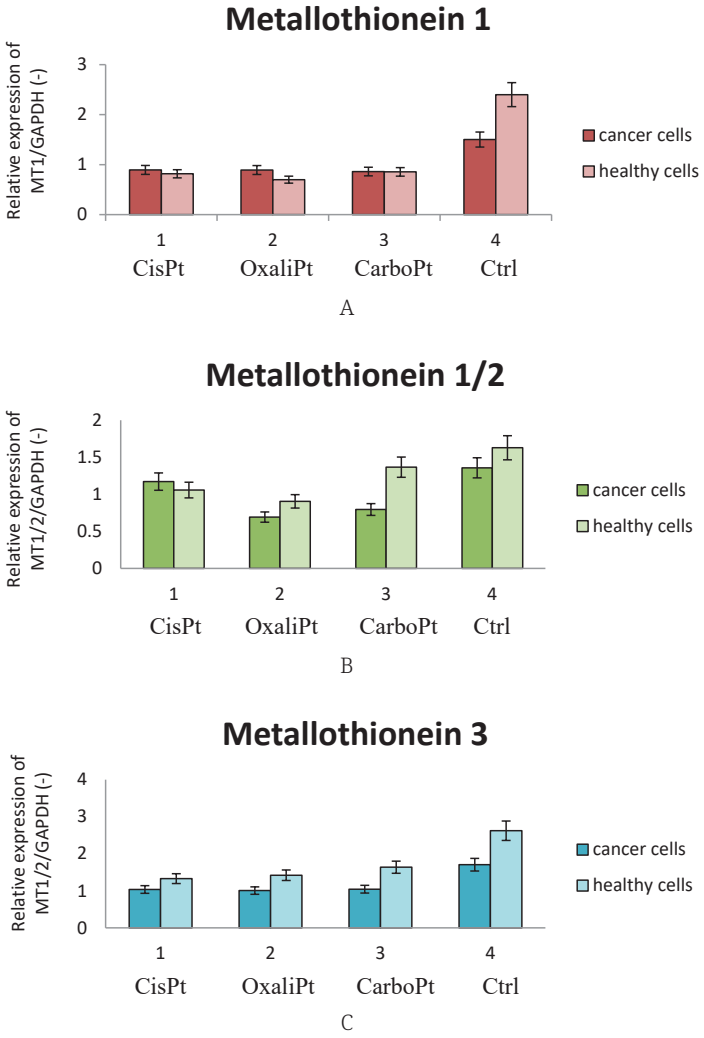

D	Cancer cells	Healthy cells	
	1 2 3 4	1 2 3 4	
GAPDH	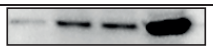		37kDa
MT1		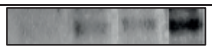	50kDa
MT1/2		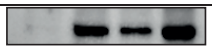	50kDa
MT3			48kDa

7: *Quantification of metallothionein 1 (A), 1/2 (B) and 3 (C) isoform expression on the protein level. D) Metallothionein bands on western blot membranes*

III: *Stylisied results of protein vs. mRNA expression*

	Healthy cells				Cancer cells			
	CisPt	OxaliPt	CarboPt	Ctrl	CisPt	OxaliPt	CarboPt	Ctrl
	Treated cells			Non-treated	Treated cells			Non-treated
mRNA expression	N/A			N/A	High			Low
Protein expression	Low			High	Low			High

GAPDH) and at similar intensities. Cancer cells matched or had slightly higher protein expression levels than healthy cells. The control, without cytostatic treatment, marked clearly higher protein expression, especially in case of healthy cells.

As we can see in Fig. 7B, the expression of proteins in case of MT1/2 for cancer cells was highest under CisPt, followed by OxaliPt and CarboPt at equal levels. The expression of proteins in healthy cells were highest under CarboPt treatment, then CisPt and OxaliPt with lowest expressions. The cells without any cytotoxic treatment showed clearly higher level of protein expressions, especially for healthy cells.

For MT3 (Fig. 7C), the expression pattern for proteins was rather similar to MT1. Cells treated with all three cytotoxics indicated almost identical expression response with healthy cells having higher protein expressions than cancer ones. The control sample without cytotoxic treatment had by far highest expression levels.

For Fig. 7D, which shows the results of the protein molecular weight we can see that the pattern corresponds to the results of the protein expression test, represented in Figs. 7A–C. All in all, the cancer cells tent to have lower protein expression than healthy cells even though there are some exceptions to this pattern, such as, CisPt and OxaliPt in MT1 and OxaliPt in MT1/2. Non-cytostatic treated cells in general showed higher protein expression than treated cells.

In a way to discuss the obtained results, we first look at the expression of mRNA and of protein. Our results show that (see Tab. III) generally speaking cells, both healthy and cancer, treated by Pt-based cytostatics manifest lower protein expression than in non-treated cells. The mRNA expression on the other hand tends to be higher for treated cancer cells but not in healthy cells. In other words, the mRNA and protein expression does not correlate. We therefore assume that presence of heavy metals – such as Pt – increase the expression of mRNA significantly more than protein expression.

The mechanism of the non-correlation of mRNA and protein level of expression remains unclear to us and requires further studies. It is worth noting that individual Pt-based cytostatics provoke slightly different expressions of mRNA and proteins. Especially CisPt and OxaliPt-based treatment in the MT1 and OxaliPt in MT1/2 resulted in higher protein expression in cancer cells than in healthy. Therefore, these MTs can protect the cells from the treatment. The phenomena of non-correlation can be explained by a protective mechanism which prevents the DNA from the methylation. Peng *et al.*. (2017) report the existence of such a mechanism which however remains unclear to them. The result of their work shows a high level of H3K4me2 in an active MT3 promoter in a specific cell line and a significantly decreased level of H3K4me2 in a suppressive promoter in OE33. This finding can help to interpret our results by suggesting that the expression of metallothionein can be slowed down compared to the expression of proteins and a mutual non-correlation can be therefore observed.

CONCLUSION

The paper focuses on expression patterns of mRNA encoding selected (sub)isoforms of MTs prior and after exposure of melanoma cells to following platinum cytostatics – cisplatin, carboplatin and oxaliplatin. MTs were also analysed at protein level using antiMT1/2 and antiMT3 antibodies. Obtained results will be compared with phenotypic response of cells (proliferation, ROS formation).

The first conclusion relates to the mortality dynamics of the healthy and cancer cells treated with Pt-based cytotoxics. The $24hIC_{50}$ for CisPt was reached at 11 μM, for OxaliPt at 1149 μM and CarboPt at 345 μM. The cell toxicity was highest for CisPt followed by CarboPt and OxaliPt.

The next result relates to oxidative stress visualized by fluorescence microscopy. After application of $24hIC_{50}$ values, the reactive oxygen species (ROS) were visually expressed. We came to the conclusion that in the healthy cells the ROS were created in the nuclei of cells treated by $24hIC_{50}$ of CisPt and OxaliPt, not CarboPt. CisPt and OxaliPt-treated cells are most stressed. CarboPt-treated cells and the control, untreated cells are a little bit less stressed.

The third set of results came from the qPCR expression of mRNA. We aimed at evaluating the quantification of expression of mRNA of three metallothionein isoforms, namely MT 1, MT 2 and

MT 3 in healthy and cancer cells exposed to 24hIC_{50} of CisPt, OxaliPt and CarboPt. Our results showed that MT 1, 2 and 3 expression manifested the highest qPCR activity after CisPt treatment (both healthy and cancer cells). We can also conclude that in principle, the platinum drug-induced overexpression of all metallothionein isoforms in cancer cells was higher compared to the one in the healthy cells.
The fourth test focused on the expression of the protein level in the healthy and cancer cells treated by the cytotoxics. Our results suggest that for MT1 and MT3, the expression of protein level under all three cytostatic treatments were low and cancer cells having higher protein expression levels as healthy cells. In case of MT1/2 for cancer cells was highest under CisPt. The expression of proteins in healthy cells were highest under CarboPt treatment. Untreated cells showed clearly higher level of protein expressions, especially for healthy cells. The cancer cells had lower protein expression than healthy cells while non-cytostatic treated cells showed a higher one than treated cells.
One important element of our study is to look on the expression of mRNA and of protein. Cells, both healthy and cancer, treated by Pt-based cytostatics manifest lower protein expression than non-treated cells. The mRNA expression did not correlate with the protein expression meaning that the cancer cells react more to the treatment on the level of mRNA expression.

Acknowledgements

The research was part of the research project *Towards the Understanding a Metal-Tumor-Metabolism*, number 115844-2, financed by ERC, project coordinator V. Adam.

REFERENCES

BUCHTELOVA, H., DOSTALOVA, S., MICHALEK, P., KRIZKOVA, S., STRMISKA, V., KOPEL, P., HYNEK, D., RICHTERA, L., RIDOSKOVA, A., ADAM, P., KYNICKY, J., BRTNICKY, M., HEGER, Z. and ADAM, V. 2017. Size-related cytotoxicological aspects of polyvinylpyrrolidone-capped platinum nanoparticles. *Food and Chemical Toxicology*, 105: 337–346.

BUCHTELOVA, H., STRMISKA, V., DOSTALOVA, S., MICHALEK, P., KRIZKOVA, S., KOPEL, P., HYNEK, D., RICHTERA, L., ADAM, V. and HEGER, Z. 2017. pH-Responsive Hybrid Organic-Inorganic Ruthenium Nanoparticles for Controlled Release of Doxorubucin. *Particle Systems Characterization*, 34(11): 1700289.

BUCHTELOVA, H., STRMISKA, V., SKUBALOVA, Z., DOSTALOVA, S., MICHALEK, P., KRIZKOVA, S., HYNEK, D., KALINA, L., RICHTERA, L., MOULICK, A., ADAM, V. and HEGER, Z. 2018. Improving cytocompability of CdTe quantum dots by Schiff-base-coordinated lanthanides surface doping. *J. Nanobiotechnol*, 16: 43.

COYLE, P., PHILCOX, J., CAREY, L. *et al.* 2002. Metallothionein: the multipurpose protein. *Cellular and Molecular Life Sciences*, 59(4): 627–647.

DICKINSON, B. C. and CHANG, C. J. 2011. Chemistry and biology of reactive oxygen species in signaling or stress responses. *Nat. Chem. Biol.*, 7(8): 504–511.

DOSTALOVA, S., CERNA, T., HYNEK, D., KOUDELKOVA, Z., VACULOVIC, T., KOPEL, P., HRABETA, J., HEGER, Z., VACULOVICOVA, M., ECKSCHLAGER, T., STIBOROVA, M. and ADAM, V. 2016. Site-Directed Conjugation of Antibodies to Apoferritin Nanocarrier for Targeted Drug Delivery to Prostate Cancer Cells. *ACS Applied Materials & Interfaces*, 8(23): 14430–14441.

DOSTALOVA, S., POLANSKA, H., SVOBODOVA, M., BALVAN, J., KRYSTOFOVA, O., HADDAD, Y., KRIZKOVA, S., MASARIK, M., ECKSCHLAGER, T., STIBOROVA, M., HEGER, Z. and ADAM, V. 2018. Prostate-Specific Membrane Antigen-Targeted Site-Directed Antibody-Conjugated Apoferritin Nanovehicle Favorably Influences in Vivo Side Effects of Doxorubicin. *Scientific Reports*, 8: 8867.

DOSTALOVA, S., VASICKOVA, K., HYNEK, D., KRIZKOVA, S., RICHTERA, L., VACULOVICOVA, M., ECKSCHLAGER, T., STIBOROVA, M., HEGER, Z. and ADAM, V. 2017. Apoferritin as an ubiquitous nanocarrier with excellent shelf life. *International Journal of Nanomedicine*, 12: 2265–2278.

KRĘŻEL, A. and MARET, W. 2007. Different redox states of metallothionein/thionein in biological tissue. *Biochem. Journal*, 402(Pt 3): 551–558.

KRĘŻEL, A. and MARET, W. 2017. The Functions of Metamorphic Metallothioneins in Zinc and Copper Metabolism. *International Journal of Molecular Sciences*, 18(6): 1237.

KRIZKOVA, S., RYVOLOVA, M., HRABETA, J., ADAM, V., STIBOROVA, M. T. and KIZEK, R. 2012. Metallothioneins and zinc in cancer diagnosis and therapy. *Journal of Pharmaceutical and Biomedical Analysis*, 44(4): 287–301.

KRIZKOVA, S., KEPINSKA, M., EMRI, G., ECKSCHLAGER, T., STIBOROVA, M., POKORNA, P., HEGER, Z. and ADAM, V. 2018. An insight into the complex roles of metallothioneins in malignant diseases with

emphasis on (sub)isoforms/isoforms and epigenetics phenomena. *Pharmacology & Therapeutics*, 183: 90–117.

KRIZKOVA, S., KEPINSKA, M., EMRI, G., MERLOS RODRIGO, A. M., TMEJOVA, K., NERUDOVA, D., KIZEK, R. and ADAM, V. 2016. Microarray analysis of metallothioneins in human diseases — A review. *Journal of Pharmaceutical and Biomedical Analysis*, 117: 464–473.

LAI, Y.-H., KUO, C., KUO, T. M. and CHEN, H. H. W. 2018. Modulating Chemosensitivity of Tumors to Platinum-Based Antitumor Drugs by Transcriptional Regulation of Copper Homeostasis. *International Journal of Molecular Sciences*, 19(5): 1486.

LIVAK, K. J. and SCHMITTGEN, T. D. 2001. Analysis of Relative Gene Expression Data Using Real-Time Quantitative PCR and the 22DDCT Method. *Methods*, 25(4), 402–408.

MCGEE, H. M., WOODS, G. M., BENNETT, B. and CHUNG, R. S. 2010. The two faces of metallothionein in carcinogenesis: photoprotection against UVR-induced cancer and promotion of tumor survival. *Photochemical & Photobiological Sciences*, 4: 586–596.

MERLOS RODRIGO, A. M., DOSTALOVA, S., BUCHTELOVA, H., STRMISKA, V., MICHALEK, P., KRIZKOVA, S., VICHA, A., JENCOVA, P., ECKSCHLAGER, T., STIBOROVA, M., HEGER Z. and ADAM, V. 2017. Comparative gene expression profiling of human metallothionein-3 up-regulation in neuroblastoma cells and its impact on susceptibility to cisplatin. *Oncotarget*, 9: 4427–4439.

NEJDL, L., KUDR, J., MOULICK, A., HEGEROVA, D., RUTTKAY-NEDECKY, B., GUMULEC, J. *et al.* 2017. Platinium nanoparticles induce damage to DNA abd inhibit DNA replication. *PLoS One*, 12(7). e0180798.

PENG, D., HU, T.-L., JIANG, A., WASHINGTON, M. K., MOSKALUK, C. A., SCHNEIDER-STOCK, R. *et al.* 2011. Location-Specific Epigenetic Regulation of the Metallothionein 3 Gene in Esophageal Adenocarcinomas. *PLoS One*, 6(7): e22009.

SI, M. and LANG, J. 2018. The roles of metallothioneins in carcinogenesis. *Journal of Hematology & Oncology*, 11: 107.

SKOWRON, M. A., MELNIKOVA, M., VAN ROERMUND, J. G. H., ROMANO, A., ALBERS, P., THOMALE, J., SCHULZ, W. A., NIEGISCH G. and HOFFMANN, M. J. 2018. Multifaceted Mechanisms of Cisplatin Resistance in Long-Term Treated Urothelial Carcinoma Cell Lines. *International Journal of Molecular Sciences*, 19(2): 590.

WONG, D. L. and STILLMAN, M. J. 2018. Capturing platinum in cisplatin: kinetic reactions with recombinant human apo-metallothionein 1a. *Metallomics*, 10: 713–721.

ZALEWSKA, M., TREFON, J. and MILNEROWICZ, H. 2014. The role of metallothionein interactions with other proteins. *Proteomics*, 14(11): 1343–1356.

Contact information

Sofie Blížkovská: sofie.bliz@hotmail.fr